EARTHQUAKE ENGINEERING AND STRUCTURAL DYNAMICS
Earthquake Engng Struct. Dyn. 2003; **32**:1201–1215 (DOI: 10.1002/eqe.268)

Hybrid platform for vibration control of high-tech equipment in buildings subject to ground motion. Part 2: Analysis

Z. C. Yang[1], Y. L. Xu[2,*,†], J. Chen[2] and H. J. Liu[1]

[1] *Department of Aircraft Engineering, Northwestern Polytechnical University, Xi'an 710072, China*
[2] *Department of Civil and Structural Engineering, The Hong Kong Polytechnic University, Kowloon, Hong Kong, China*

SUMMARY

The experimental results of using a hybrid platform to mitigate vibration of a batch of high-tech equipment installed in a building subject to nearby traffic-induced ground motion have been presented and discussed in the companion paper. Based on the identified dynamic properties of both the building and the platform, this paper first establishes an analytical model for hybrid control of the building-platform system subject to ground motion in terms of the absolute co-ordinate to facilitate the absolute velocity feedback control strategy used in the experiment. The traffic-induced ground motion used in the experiment is then employed as input to the analytical model to compute the dynamic response of the building-platform system. The computed results are compared with the measured results, and the comparison is found to be satisfactory. Based on the verified analytical model, coupling effects between the building and platform are then investigated. A parametric study is finally conducted to further assess the performance of both passive and hybrid platforms at microvibration level. The analytical study shows that the dynamic interaction between the building and platform should be taken into consideration. The hybrid control is effective in reducing both velocity response and drift of the platform/high-tech equipment at microvibration level with reasonable control force. Copyright © 2003 John Wiley & Sons, Ltd.

KEY WORDS: analytical study; high-tech equipment; microvibration; nearby traffic-induced ground motion; hybrid platform; comparison; coupling effects

1. INTRODUCTION

Most of the studies for protecting high-tech equipment from building floor vibration are concerned with vibration isolation systems. These vibration isolation systems include passive mounts, hybrid tables and active tables that are mainly used for isolating individual or a small

* Correspondence to: Y. L. Xu, Department of Civil and Structural Engineering, The Hong Kong Polytechnic University, Hung Hom, Kowloon, Hong Kong, China.
† E-mail: ceylxu@polyu.edu.hk

Contract/grant sponsor: Hong Kong Research Grants Council, and Hong Kong Polytechnic University.

Received 15 August 2002
Accepted 29 September 2002

Copyright © 2003 John Wiley & Sons, Ltd.

quantity of high-tech equipment [1–3]. The analytical model of the concerned problem often takes building floor vibration as a direct base excitation to the vibration isolation system [1]. The high-tech equipment together with the vibration isolation table, if any, are often modelled as a rigid body and occasionally as an elastic body [4]. The degrees of freedom of the rigid body or the vibration isolation system in the analytical model range from 1 to 6. Dynamic interaction between the building and the high-tech equipment/vibration isolation system, however, is not considered. Although this treatment may be adequate for a large building with limited amount of high-tech equipment, it is not sufficient and economic for a large building with a batch of high-tech equipment, as evidenced in many modern high-tech facilities subject to nearby traffic-induced ground motion.

Recently, Yang and Agrawal [5] performed an extensive theoretical study on the possible use of various protective systems for vibration control of high-tech facilities under nearby traffic-induced ground motion in consideration of dynamic interaction between the control system and building. The protective systems that they investigated included passive building base isolation, hybrid building base isolation, passive floor isolation, hybrid floor isolation, active control systems and passive energy dissipation systems. They concluded that hybrid floor isolation could be the most effective and practical means in satisfying the design specification for vibration of high-tech equipment. However, in their investigation the governing equation of motion of the building with protective systems was established in terms of relative motion to the ground, and the controller was designed based on the drift and relative velocity of the floor isolator. The use of relative velocity as feedback to control the absolute velocity of the floor may not be compatible. Furthermore, there were no experimental results supporting their findings.

This paper, together with the companion paper [6] presents a combined experimental and analytical study, considering the coupled building-platform system, to examine the effectiveness of a hybrid platform for mitigating vibration of a batch of high-tech equipment installed in a building subject to nearby traffic-induced ground motion. Based on the dynamic properties of the building and the platform identified in the companion paper, this paper first establishes an analytical model for hybrid control of the building-platform system subject to ground motion in terms of the absolute co-ordinate to facilitate the absolute velocity feedback control strategy used in the experiment. The traffic-induced ground motion measured in the experiment is then employed as input to the analytical model to compute the dynamic responses of both the building and hybrid platform of different parameters. The computed results are compared with the measured results. Based on the verified analytical model, coupling effects between the building and platform are then investigated. An extensive parametric study is finally conducted to further assess the performance of both passive and hybrid platforms at microvibration level.

2. ANALYTICAL MODEL

2.1. System identification of building and platform

To establish an analytical model for the hybrid control of the building-platform system tested in the companion paper, the mass, stiffness and damping matrices of the building itself are first formed based on the measured data. The weights of the building components and the

Copyright © 2003 John Wiley & Sons, Ltd.

Table I. Comparison of velocity response of the hybrid platform.

Control gain (%)	Anal. max. vel. (mm/s)	Exp. max. vel. (mm/s)	Rel. diff. (%)	Anal. rms vel. (mm/s)	Exp. rms vel. (mm/s)	Rel. diff. (%)
20	35.56	29.17	17.96	9.19	7.77	15.47
40	29.80	27.18	8.79	8.15	7.46	8.37
60	25.82	25.50	1.25	7.47	7.27	2.73
80	24.02	24.43	−1.71	6.87	7.00	−1.85
100	21.93	21.49	2.00	6.25	6.70	−7.23

weight of the actuator were measured and calculated to form the mass matrix of the building model, which is regarded as a diagonal matrix.

$$[M] = \begin{bmatrix} 100.7 & 0 & 0 \\ 0 & 100.7 & 0 \\ 0 & 0 & 91.8 \end{bmatrix} (\text{kg}) \tag{1}$$

The stiffness and damping matrices of the building can be identified based on the measured three natural frequencies, three normalized modal shapes and three modal damping ratios of the building without the platform, as listed in Table I in the companion paper [6], using the following equations [7].

$$[K] = [M][\Phi][\text{diag}(\omega_i^2/\bar{m}_i)][\Phi]^{\text{T}}[M] \tag{2}$$

$$[C] = [M][\Phi][\text{diag}(2\zeta_i\omega_i/\bar{m}_i)][\Phi]^{\text{T}}[M] \tag{3}$$

where $[\Phi]$ is the measured 3×3 mode shape matrix; ω_i is the measured ith natural frequency of the building without the platform; ζ_i is the measured ith modal damping ratio of the building without the platform; and $\bar{m}_i$ is the ith generalized mass of the building without the platform.

The stiffness and damping matrices identified for the building itself are then given by

$$[K] = \begin{bmatrix} 3.5322 & -1.9364 & 0.2102 \\ -1.9364 & 3.4895 & -1.8079 \\ 0.2102 & -1.8079 & 1.6751 \end{bmatrix} \times 10^6 \ (\text{N/m}) \tag{4}$$

$$[C] = \begin{bmatrix} 95.26 & -32.74 & 5.75 \\ -32.74 & 96.69 & -28.57 \\ 5.75 & -28.57 & 64.37 \end{bmatrix} (\text{Ns/m}) \tag{5}$$

The identified stiffness and damping matrices indicate that the building model used in the experiment can be approximately regarded as a shear-type building. The weight of the

Copyright © 2003 John Wiley & Sons, Ltd.

Table II. Comparison of velocity response of building second floor.

Control gain (%)	Anal. max. vel. (mm/s)	Exp. max. vel. (mm/s)	Rel. diff. (%)	Anal. rms vel. (mm/s)	Exp. rms vel. (mm/s)	Rel. diff. (%)
20	32.21	33.35	−3.55	9.19	9.11	0.88
40	31.72	31.09	1.99	9.47	8.45	10.77
60	33.97	31.09	8.47	9.78	8.22	15.97
80	33.36	30.11	9.73	10.07	8.16	19.01
100	35.02	30.66	12.44	10.37	8.30	19.94

platform together with its accessories was measured as 20.5 kg. The stiffness of the platform can be determined in terms of the measured natural frequency and mass of the platform. The damping coefficient of the platform can be calculated based on the measured natural frequency and damping ratio of the platform, as listed in Table II in the companion paper [6].

2.2. Governing equation of motion

In consideration that the feedback control and the control performance evaluation of the hybrid platform are based on its absolute velocity in the experiment, the governing equation of motion of the hybrid platform-building system is established in the absolute co-ordinate system.

$$\begin{bmatrix} m_{11} & 0 & 0 & 0 \\ 0 & m_{22} & 0 & 0 \\ 0 & 0 & m_{33} & 0 \\ 0 & 0 & 0 & m_{\mathrm{p}} \end{bmatrix} \begin{Bmatrix} \ddot{x}_1 \\ \ddot{x}_2 \\ \ddot{x}_3 \\ \ddot{x}_{\mathrm{p}} \end{Bmatrix} + \begin{bmatrix} c_{11} & c_{12} & c_{13} & 0 \\ c_{21} & c_{22}+c_{\mathrm{p}} & c_{23} & -c_{\mathrm{p}} \\ c_{31} & c_{32} & c_{33} & 0 \\ 0 & -c_{\mathrm{p}} & 0 & c_{\mathrm{p}} \end{bmatrix} \begin{Bmatrix} \dot{x}_1 \\ \dot{x}_2 \\ \dot{x}_3 \\ \dot{x}_{\mathrm{p}} \end{Bmatrix}$$

$$+ \begin{bmatrix} k_{11} & k_{12} & k_{13} & 0 \\ k_{21} & k_{22}+k_{\mathrm{p}} & k_{23} & -k_{\mathrm{p}} \\ k_{31} & k_{32} & k_{33} & 0 \\ 0 & -k_{\mathrm{p}} & 0 & k_{\mathrm{p}} \end{bmatrix} \begin{Bmatrix} x_1 \\ x_2 \\ x_3 \\ x_{\mathrm{p}} \end{Bmatrix} = \begin{Bmatrix} 0 \\ -f_{\mathrm{c}} \\ 0 \\ f_{\mathrm{c}} \end{Bmatrix} + \begin{Bmatrix} c_{11}/2 \\ 0 \\ 0 \\ 0 \end{Bmatrix} \dot{x}_{\mathrm{g}} + \begin{Bmatrix} k_{11}/2 \\ 0 \\ 0 \\ 0 \end{Bmatrix} x_{\mathrm{g}} \quad (6)$$

where m_{ii}, k_{ij} and c_{ij} $(i=1,2,3;\ j=1,2,3)$ are the mass, stiffness coefficient and damping coefficient of the building without the platform directly adopted from Equations (1), (4) and (5), respectively; m_{p}, k_p and c_{p} are the mass, stiffness coefficient and damping coefficient of the platform, respectively; $x_i, \dot{x}_i$ and $\ddot{x}_i$ $(i=1,2,3,p)$ are the horizontal absolute displacement, velocity and acceleration, respectively, of either the ith building floor or the platform with respect to the earth; f_{c} is the control force generated by the actuator; x_{g} and $\dot{x}_{\mathrm{g}}$ are the displacement and velocity of the ground motion in the horizontal direction, respectively. The displacement and velocity of the ground motion can be obtained by integrating the ground acceleration time history with the time. To eliminate the shift of velocity and displacement

Copyright © 2003 John Wiley & Sons, Ltd.

time histories during the integration, the ground acceleration time history is passed through a proper high-band filter before the integration. Equation (6) can be converted to the state space as

$$\{\dot{z}\} = [A]\{z\} + \{B\}f_c + \{E_1\}\dot{x}_g + \{E_2\}x_g \tag{7}$$

where $\{z\} = \{x_1\ x_2\ x_3\ x_p\ \dot{x}_1\ \dot{x}_2\ \dot{x}_3\ \dot{x}_p\}^T$ is the state vector of the building-platform system; $[A]_{8\times 8}$ is the state matrix; $\{B\}_{8\times 1}$ is the control vector; and $\{E_1\}_{8\times 1}$ and $\{E_2\}_{8\times 1}$ are the two influence vectors related to the ground motion.

2.3. Control strategy

Because traffic-induced ground motion should be considered as a frequent event, the main concern is thus to reduce the velocity response of the platform for the normal operation of high-tech equipment to ensure the quality of ultra-precision products [8]. In this connection, the reduction of absolute velocity response of the platform is targeted in the design of the hybrid platform. From a practical point of view, it is difficult, if not impossible, to measure the response of all the building floors and the platform. The sub-optimal control strategy is adopted in the analytical study to be consistent with that used in the experiment. The sub-optimal control strategy uses the absolute velocity of the platform as a feedback variable. The relation between the original state vector $\{z\}$ and the measurement vector $\{y\}$ is expressed as

$$y = \dot{x}_p = [C]\{z\} \tag{8}$$

where $[C] = [0\ 0\ 0\ 0\ 0\ 0\ 0\ 1]$ called the measurement matrix.

Using the minimum norm method of the sub-optimal control theory [9], the sub-optimal control force is determined by

$$f_c = -[F]y = -[F][C]\{z\} \tag{9}$$

where

$$[F] = [K][C]^T([C][C]^T)^{-1} \tag{10}$$

in which $[K]$ is the optimal constant feedback gain matrix obtained by the minimizing the performance function

$$J = \frac{1}{2}\int_0^\infty (\{z\}^T[Q]\{z\} + f_c R f_c)\,dt \tag{11}$$

subjected to the constraint of Equation (7). The matrix $[Q]$ is the positive semi-definite weighting matrix for the state vector $\{z\}$ and the scalar R is the positive weight factor for the control force f_c. By selecting appropriate $[Q]$ and R, the sub-optimal feedback gain matrix $[F]$ can be determined. Then, Equations (7) and (9) are solved simultaneously using the fourth-order Rung–Kutta method provided in the MATLAB-Similink.

Copyright © 2003 John Wiley & Sons, Ltd.

Table III. Comparison of drift of the hybrid platform.

Control gain (%)	Anal. max. drift (mm)	Exp. max. drift (mm)	Rel. diff. (%)	Anal. rms drift (mm)	Exp. rms drift (mm)	Rel. diff. (%)
20	1.09	1.04	4.58	0.30	0.28	6.65
40	1.04	0.89	14.66	0.28	0.25	9.51
60	0.96	0.82	14.38	0.26	0.23	12.80
80	0.91	0.74	18.62	0.25	0.21	18.42
100	0.83	0.68	18.32	0.24	0.19	20.56

3. COMPARISON WITH EXPERIMENTAL RESULTS

For a given platform stiffness and platform damping ratio, the absolute velocity response and drift response of the hybrid platform and the absolute velocity response of the second floor of the building are computed for different control gains using Equations (7) and (9) as well as the nearby traffic-induced ground acceleration time history recorded in the experiment as shown in Figure 3 in the companion paper [6]. The control gains used in the experiment between the absolute velocity of the platform and the control force are from 20 to 100% of the nominal control gain of 640 N s/m at an interval of 20%. The peak acceleration of the nearby traffic-induced ground motion used in the experiment is $0.06g$, where g is the acceleration due to gravity.

Listed in Table I are the analytical and experimental results of the absolute maximum and rms velocity responses of the hybrid platform for stiffness case $D1$ and damping case $C3$ (refer to the companion paper [6]). Both analytical and experimental results manifest that with increasing control gain, the maximum and rms velocity responses of the hybrid platform decrease. The mean value of relative differences between the analytical and experimental results, taking the analytical results as a basis is 5.66% for the maximum velocity and 4.23% for the rms velocity. Displayed in Table II are the analytical and experimental results of the absolute maximum and rms velocity responses of the second floor of the building for stiffness case $D1$ and damping case $C3$. It is seen that the velocity response of the second floor of the building changes slightly with control gain. The mean values of relative differences between the analytical and experimental maximum and rms responses are 5.82 and 13.3%, respectively. The analytical and experimental results of the maximum and rms drifts of the hybrid platform are tabulated in Table III for stiffness case $D1$ and damping case $C3$. The mean value of relative differences between analytical and experimental results is 14.0% for the maximum drift and 13.6% for the rms drift. Figure 1 shows the comparison of velocity response time history of the hybrid platform between the experiment and analysis. The control gain, the stiffness case, and the damping case are 100%, $D1$ and $C3$, respectively. It is seen that the computed response time history is very similar to the measured response time history.

In summary, the comparison between the experimental and analytical results is satisfactory in general. There are some cases in which the differences between the analytical and experimental results are around 20%. Such differences are attributed to many factors. Among them

Copyright © 2003 John Wiley & Sons, Ltd.

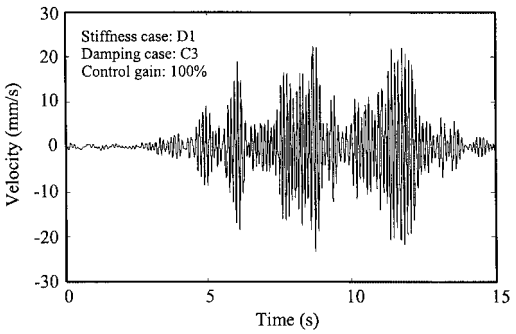

(a) Computed time history

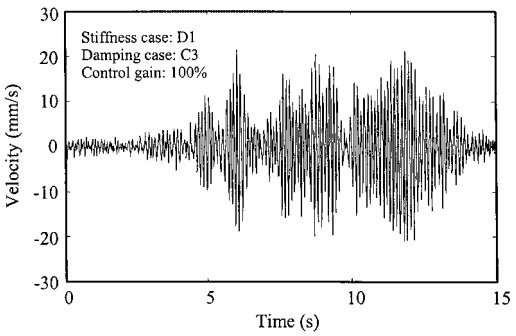

(b) Measured time history

Figure 1. Comparison of absolute velocity response time histories of platform.

are uncertainties in the identification of modal damping ratios of either the building or the platform, the measurement noise in the experimental results, the deviation of platform stiffness from linear status due to larger deformation, and the frequency dependence of control force generated by the actuator.

4. COUPLING EFFECTS

As mentioned in the introduction, the dynamic interaction (coupling effect) between the building and the platform either passively isolated or actively controlled is not considered in most of the previous studies. Such coupling effects are now investigated using the verified analytical model. To demonstrate the coupling effects between the building and platform, the absolute displacement and velocity responses of the second floor of the building without the platform under the traffic-induced ground acceleration are first computed. The obtained displacement and velocity response time histories are then taken as ground excitations and input directly into the base of the platform to determine the absolute velocity response of the platform. The velocity responses of the platform and the second floor of the building without the platform obtained in such a way are finally compared with those obtained from the coupled building and platform system under the same traffic-induced ground motion.

Copyright © 2003 John Wiley & Sons, Ltd.

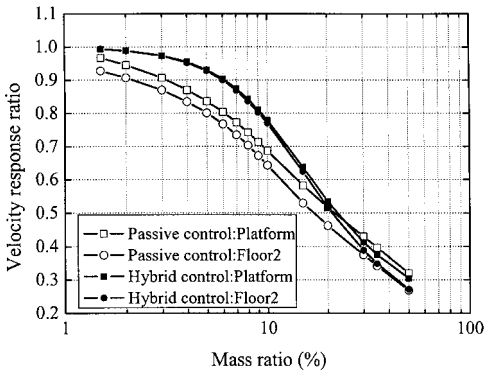

Figure 2. Coupling effects of the system with higher frequency platform.

In this exercise, the building model and the ground motion are the same as those used in the experiment. The mass of either the passive platform or the hybrid platform varies from 1.5 to 50% of the mass of the building second floor. The stiffness of the platform also varies in such a way that the frequency of the platform is kept as a constant of 6.15 Hz. The damping ratio and the velocity feedback control gain of the platform remain unchanged at 10% and 640 N s/m, respectively. The absolute velocity responses of the platform and the second floor of the building computed from the coupled building-platform system are divided by the corresponding responses of the uncoupled platform and the uncoupled second floor of the building to obtain the normalized velocity responses (velocity response ratios). Figure 2 displays the velocity response ratios of the passive platform, the hybrid platform and the corresponding second floor of the building against the mass ratio for the platform frequency of 6.15 Hz. The mass ratio here is defined as the mass of the platform to the mass of the building second floor. It is seen that all the normalized velocity responses decrease with increasing mass ratio. For the hybrid platform, if the mass ratio is less than 6%, the separated computation (uncoupled approach) overestimates the velocity responses of both the hybrid platform and the building second floor by less than 10%. However, if the mass ratio reaches 20% the separated computation may overestimate the velocity responses of both the hybrid platform and the second building floor by 50%. For the passive platform, the dynamic interaction (coupling effects) between the platform and the building is quite significant. At a mass ratio of 6%, the separated computation overestimates the velocity responses of both the passive platform and the building second floor by 20%. Therefore, one may conclude that when a batch of high-tech equipment is installed on the common platform either passively isolated or actively controlled, the coupling effects must be taken into consideration. The experiment or the computation must be conducted based on the coupled building-platform system.

According to the time scale used in the shaking table test in the companion paper, the natural frequency of the platform of 6.15 Hz corresponds to 2.36 Hz for a prototype platform. A lower natural frequency of 2.0 Hz corresponding to 0.77 Hz for a prototype platform is used to further examine the coupling effects between the platform and the building. All the other parameters remain the same as those used in the case of the natural frequency of 6.15 Hz. The computation results are plotted in Figure 3. Compared with the results in Figure 2, it can be

Copyright © 2003 John Wiley & Sons, Ltd.

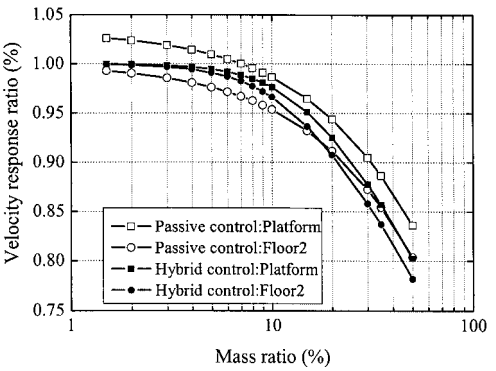

Figure 3. Coupling effects of the system with lower frequency platform.

seen that the coupling effects between the building and platform are much weaker when the natural frequency of the platform is reduced to 2 Hz. Under such an isolation frequency, when the mass ratio is less than 7% the separated computation (uncoupled approach) underestimates the velocity response of the passive platform by less than 4% but overestimates the velocity response of the building second floor by less than 5%. For the hybrid platform, the normalized responses of both the hybrid platform and the second floor are equal to almost one when the mass ratio is less than 4%, which indicates that there are almost no coupling effects between the building and the hybrid platform. However, when the mass ratio is larger than 10%, the normalized velocity responses of the passive platform, the hybrid platform, and the building second floor become smaller and smaller with increasing mass ratio. The coupling effects become more and more significant. The separated computation overestimates the responses of both the building and platform considerably.

5. PARAMETRIC STUDY AT MICROVIBRATION LEVEL

All the above studies use the nearby traffic-induced ground acceleration measured in the shake table test of 0.06g peak acceleration because of the limitation of the experimental equipment. Such high ground acceleration may not be subjected to high-tech facilities in real situations. Therefore, the following parametric study is performed using a much smaller traffic-induced ground motion for the verified analytical model at microvibration level. By trial and error, the peak acceleration of the nearby traffic-induced ground motion input to the analytical model is finally selected as 0.003g. The duration, the sampling frequency, and the other parameters of the simulated ground acceleration time history remain the same as the one used in the shaking table test.

5.1. BBN vibration criteria for high-tech equipment

Several well-known families of generic vibration criteria are in use for microvibration control of high-tech equipment [10]. The Bolt Beranek & Newman (BBN) vibration criteria may be

Copyright © 2003 John Wiley & Sons, Ltd.

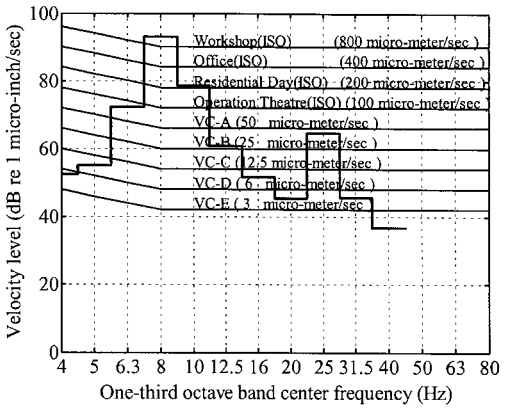

Figure 4. Velocity spectrum of second floor of building without control.

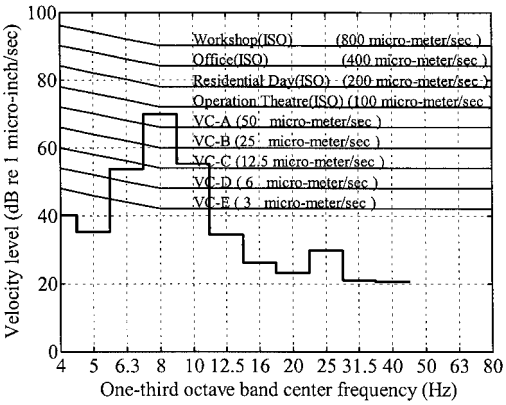

Figure 5. Velocity spectrum of passive platform.

one of the most popular criteria used in practice. The BBN vibration criteria [10, 11] for high-tech equipment take the form of a set of one-third octave band velocity spectra labelled with vibration criterion curves from VC-A to VC-E, as shown in Figures 4–7, in which the velocity spectrum is expressed in dB referenced to 1 μin/s. The curves VC-A to VC-E correspond to the allowable rms velocity from 2000 μin/s (50 μm/s) to 125 μin/s (3 μm/s) within a frequency range between 8 and 80 Hz. The International Standard Organization (ISO) guidelines for the effects of vibration on people in buildings are also plotted in these figures for reference.

Since the BBN vibration criteria are used in this study to evaluate the control performance, the absolute velocity response time histories of either the platform or the second floor of the building should be converted to the one-third octave plots. The one-third octave plot of any velocity response time-history $\dot{x}(t)$ can be obtained from its Fourier transform $\dot{X}(n)$ [12] in

Copyright © 2003 John Wiley & Sons, Ltd.

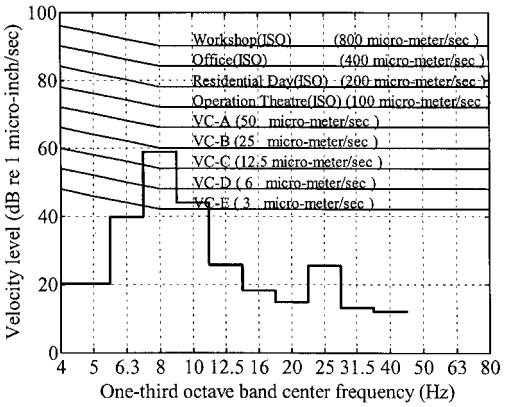

Figure 6. Velocity spectrum of hybrid platform.

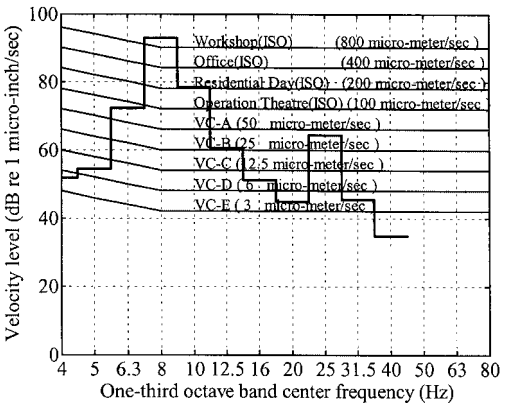

Figure 7. Velocity spectrum of second floor of building with hybrid platform.

approximation using the following equation:

$$\dot{X}_{1/3}(n_c) = \left[\sum_{0.89n_c}^{1.12n_c} |\dot{X}(n)|^2 \Delta n \right]^{1/2} \tag{12}$$

where Δn is the resolution of FFT; n is the frequency in Hz; and n_c is the centre frequency. The centre frequency is given by $n_c = 2^{(m/3)}$, where m is an integer. The one-third octave bandwidth is approximately 23% of its centre frequency. Clearly, the one-third octave plot obtained from Equation (12) is constant in the frequency band from $0.89n_c$ to $1.12n_c$. Thus it can be plotted as a histogram. In order to evaluate $\dot{X}_{1/3}(n_c)$ in terms of the BBN vibration criteria, $\dot{X}_{1/3}(n_c)$ is also expressed in dB referenced to $V_0 = 1\ \mu$in/s, that is $V(n_c) = 20 \log_{10}[\dot{X}_{1/3}(n_c)/V_0]$.

Copyright © 2003 John Wiley & Sons, Ltd.

5.2. Microvibration control performance

The nearby traffic-induced ground motion of $0.003g$ peak acceleration is now used as input to the verified analytical model to compute the absolute velocity responses of the building without the platform, the building with the passive platform and the building with the hybrid platform. The mass, natural frequency and damping ratio of the passive platform are taken as 20.5 kg, 2.0 Hz and 10%, respectively.

For the building without any control measures, the absolute velocity response time history of the building second floor obtained from the simulation is converted to the one-third octave plot (the velocity response spectrum). The velocity response spectrum of the second floor is then compared with the BBN vibration criteria, as shown in Figure 4. It is observed that the vibration level of the second floor exceeds the specifications not only for any type of high-tech equipment but also for the effects of vibration on people in buildings. The high vibration level of the second floor occurs around the first natural frequency of the building of 8.64 Hz. The maximum velocity is 93.1dB with reference to 1 μ in/s. Clearly, the high vibration level of the building without any control measures cannot satisfy the specification for high-tech equipment.

For the building with the passive platform, the high-tech equipment is supposed to be installed on the platform. Thus, the velocity response spectrum of the passive platform is plotted in Figure 5 compared with the velocity response spectrum of the second floor of the building shown in Figure 4. It is seen that the maximum velocity response is reduced to 70 dB with respect to 1 μ in/s and also occurs around the first natural frequency of the building. Although the maximum velocity response of the passive platform exceeds the specification for any type of high-tech equipment, it satisfies the ISO specifications for human comfort for a variety of structures.

When the hybrid platform is installed on the second floor of the building with velocity feedback control, the maximum velocity response of the platform is further reduced to 58 dB with reference to 1 μ in/s, as demonstrated in Figure 6. The hybrid platform of such a microvibration level can now accommodate the VC-A and VC-B type high-tech equipment though it still does not satisfy the requirement for the VC-C to VC-E type high-tech equipment. The maximum control force required for achieving such a vibration reduction is less than 0.05% of the weight of the second floor of the building. The effect of the installation of the hybrid platform on the building is also assessed here. In this connection, the velocity response of the second floor of the building with the hybrid platform is computed and converted to the one-third octave plot, as shown in Figure 7. Compared with the velocity response of the spectrum of the second floor of the building without the platform shown in Figure 4, one may see that the two velocity response spectra are very close to each other, indicating that the installation of the hybrid platform does not affect the velocity response of the building.

5.3. Parametric study

An extensive parametric study is carried out to see variations of the control performance of both the passive and hybrid platforms with two major parameters: platform frequency and damping ratio. The control performance is assessed in terms of the maximum velocity response, the maximum drift of the platform, and the control force in the case of hybrid control.

Copyright © 2003 John Wiley & Sons, Ltd.

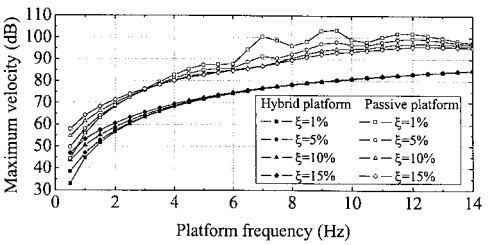

Figure 8. Variations of maximum velocity of platform with frequency.

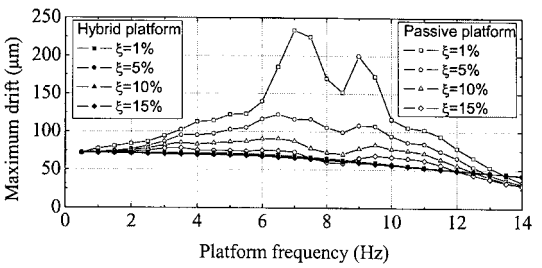

Figure 9. Variations of maximum drift of platform with frequency.

Figure 8 depicts the maximum velocity responses of both the passive platform and hybrid platform against platform frequency and damping ratio. The maximum velocity responses displayed in Figure 8 are in dB identified from the corresponding velocity response spectra. Clearly, the velocity response of the hybrid platform is much smaller than that of the passive platform over a wide range of frequency and damping ratio. With increasing platform frequency, the maximum velocity response of the platform increases in general. For the hybrid platform, the damping ratio of the platform does not affect the maximum velocity response except when the frequency of the platform is small, where smaller damping ratio leads to relatively larger vibration reduction. For the passive platform, when the platform frequency is above 3 Hz, the higher damping ratio of the platform results in relatively lower platform vibration. However, the situation is reversed when the frequency of the platform is below 3 Hz. Figure 9 displays the platform drift against the natural frequency and damping ratio of the platform. It is interesting to see that the maximum drift of the hybrid platform decreases slightly with increasing frequency of the platform. It is also insensitive to the damping ratio of the platform. For the passive platform of the small damping ratio, when the platform frequency approaches the first natural frequency of the building, the platform drift is extremely large. With increasing damping ratio of the platform, the platform drift decreases significantly. When the damping ratio is increased to 15%, the drift level of the passive platform is similar to that of the hybrid platform. Furthermore, Figure 10 shows the control force required for achieving microvibration reduction of the hybrid platform presented in Figures 8 and 9 against the frequency and damping ratio of the platform with a fixed control feedback gain. It is seen that the required control force increases with increasing frequency of the platform but it is almost independent of the damping ratio of the platform. Even with the

Copyright © 2003 John Wiley & Sons, Ltd.

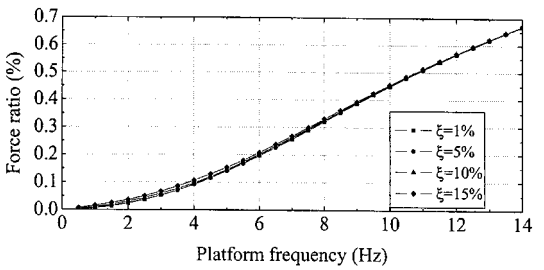

Figure 10. Variations of maximum control force with frequency.

higher frequency of the platform of 10 Hz, the required control force is less than 0.5% of the weight of the second floor of the building. From the combination of the results presented in Figures 8–10, one may conclude the hybrid control is superior to the passive platform in reducing both the velocity response and drift of the platform/high-tech equipment with reasonable control force. The control performance of the hybrid platform is also less sensitive to the damping ratio than the passive platform. The installation of the hybrid platform does not amplify the building response.

6. CONCLUSIONS

Based on the identified dynamic properties and the measured responses of both the building and platform in the companion paper [6], the analytical model for hybrid control of the building-platform system subject to nearby traffic-induced ground motion has been established and verified. By using the verified analytical model, the coupling effects between the building and platform have been investigated, and the performance of the hybrid platform has been assessed at microvibration level. The computation results demonstrate that the coupling effects between the building and platform were significant and should be taken into consideration, in particular when the natural frequency of the platform is high. The hybrid control was superior to the passive platform in reducing both the velocity response and drift of the platform/high-tech equipment with reasonable control force. The control performance of the hybrid platform was also less sensitive to the damping ratio than the passive platform, and the installation of the hybrid platform did not amplify the building response.

ACKNOWLEDGEMENTS

The authors are grateful for the financial support from the Hong Kong Research Grants Council through a CERG grant (PolyU 5054/02E and from the Hong Kong Polytechnic University through its Area of Strategic Development Programme in Structural Control.

REFERENCES

1. Nakamura Y, Nakayama M, Masuda K, Tanaka K, Yasuda M, Fujita T. Development of 6-DOF microvibration control system using giant magnetostrictive actuator. In *Proceedings of the SPIE*, Washington, U.S.A., vol. 3671, 1999; 229–240.

Copyright © 2003 John Wiley & Sons, Ltd.

2. Serrand M, Elliott SJ. Multichannel feedback control for the isolation of base-excited vibration. *Journal of Sound and Vibration* 2000; **234**(4):681–704.
3. Yoshioka H, Takahashi Y, Katayama K, Imazwa T, Murai N. An active microvibration isolation system for hi-tech manufacturing facilities. *Journal of Vibration and Acoustics* (ASME) 2001; **123**:269–275.
4. Yoshioka H, Murai N, Abe T, Hashimoto Y. Active microvibration control system by considering elastic deformation modes of vibration isolation table. *Proceedings of the 15th International Modal Analysis Conference*. SEM: Tokyo, Japan, 1997; 92–97.
5. Yang JN, Agrawal AK. Protective systems for high-technology facilities against microvibration and earthquake. *Journal of Structural Engineering and Mechanics* 2000; **10**(6):561–567.
6. Xu YL, Liu HJ, Yang ZC. Hybrid platform for vibration control of high-tech equipment in buildings subject to ground motion. Part 1: Experiment. *Earthquake Engineering and Structural Dynamics* 2003; **32**:1185–1200.
7. Xu YL, Zhan S, Ko JM, Zhang WS. Experimental investigation of adjacent buildings connected by fluid damper. *Earthquake Engineering and Structural Dynamics* 1999; **28**:609–631.
8. Ungar EE, Sturz DH, Amick CH. Vibration control design of high-technology facilities. *Sound and Vibration* 1990; **24**(7):20–27.
9. Kosut RL. Sub-optimal control of the linear time-invariant systems subject to control structure constraints. *IEEE Transactions on Automatic Control* 1970; **15**(5):557–563.
10. Amick H. On the generic vibration criteria for advanced technology facilities. *Journal of the Institute of Environmental Sciences* 1997; **XL**(5):35–44.
11. Gordon CG. Generic criteria for vibration sensitive equipment. In *Proceedings of the SPIE*, Washington, U.S.A., vol. 1619, 1991; 71–85.
12. Amick H, Bui SK. A review of several methods for processing vibration data. In: *Proceedings of the SPIE*, Washington, U.S.A., vol. 1619, 1991; 253–264.

Copyright © 2003 John Wiley & Sons, Ltd.